



Fellenius, B.H., Edvardsson, F., Pettersson, J., Sabbatini, M., and Wallgren, J, 2019. Prediction, testing, and analysis of a 50 m long pile in soft marine clay. *Journal of the Deep Foundation Institute*, 13(2) 1-7.

Prediction, Testing, and Analysis of a 50 m Long Pile in Soft Marine Clay

Bengt H. Fellenius^{1*}, Fredrik Edvardsson², Johannes Pettersson³, Michael Sabattini⁴, and Johnny Wallgren⁵

Abstract: On April 4, 2018, 209 days after driving, a static loading test was performed on a 50 m long, strain-gage instrumented, square 275-mm diameter, precast, shaft-bearing (“floating”) pile in Göteborg, Sweden. The soil profile consisted of a 90 m thick, soft, postglacial, marine clay. The groundwater table was at about 1.0 m depth. The undrained shear strength was about 20 kPa at 10 m depth and increased linearly to about 80 kPa at 55m depth. The load-distribution at the peak load correlated to an average effective stress beta-coefficient of 0.19 along the pile or, alternatively, a unit shaft shear resistance of 15 kPa at 10 m depth increasing to about 65 kPa at 50 m depth, indicating an α -coefficient of about 0.80. Prior to the test, geotechnical engineers around the world were invited to predict the load-movement curve to be established in the test—22 predictions from 10 countries were received. The predictions of pile stiffness, and pile head displacement showed considerable scatter, however. Predicted peak loads ranged from 65% to 200% of the actual 1,800-kN peak-load, and 35% to 300% of the load at 22-mm movement.

Keywords: *static loading test, precast concrete pile, strain-gage instrumentation, axial stiffness, stress-dependent and stress-independent shaft resistance*

Introduction

Performing static loading tests is rather rare in current Swedish engineering practice, piles mostly being toe-bearing in very competent soil. However, in connection with an ongoing construction in central Göteborg, Sweden, involving tall buildings and highway viaducts supported on shaft-bearing (“floating”) piles, a static load test was carried out on a 50 m long, strain-gage instrumented, square 275-mm diameter, precast pile. We believe that the tests results are of some general interest.

The event offered the opportunity to invite the profession to predict the load-movement response of ahead of the test. Over the years, many such professional events have been carried out—some very elaborate and others rather casual. Although the primary purpose of most of these events was for

entertainment at a deep foundation conference, the compilation of the predictions submitted for the current case are of a wider interest as they reflect on an almost palpable disparity in the state-of-practice.

This paper presents information on the soil profile at the test site, compilation of received predictions, and evaluation of the test results. The second and third authors have reported the test in a Master Thesis (Edvardsson and Pettersson, 2018) supervised by the fourth and fifth authors.

Soil Profile

The soil profile at the site is shown in Figure 1. It consists of about 3 m thick heterogeneous backfill (decades old) overlying a 90 m thick layer of homogenous, soft, normally consolidated, postglacial, marine clay overlying a few metre of glacial till on bedrock. The water content ranges from about 65% near the ground surface to about 50% at 50 m depth, corresponding to unit densities of 1,600 and 1,700 kg/m³, respectively. The liquid limit, w_L , in the clay is about 10% larger than the natural water content, w_n . The groundwater table was at about 1.0 depth. Pore-pressure measurements in stand-pipes in the glacial till some 400 m away from the test site have indicated a pressure head to about 2 m above the ground surface. As the clay is normally consolidated, the pore pressure distribution is considered linear between the glacial till and the GW level.

Test Pile

The test pile is a precast concrete pile with a 275-mm nominal diameter constructed in one 11.0 m toe-segment and three

¹ Consulting Engineer, Sidney, BC, V8L 2B9, Canada

² Project Engineer, PEAB, Nellickevägen 22, 41263 Göteborg, Sweden

³ Project Engineer, PEAB, Nellickevägen 22, 41263 Göteborg, Sweden

⁴ Project Engineer, PEAB, Nellickevägen 22, 41263 Göteborg, Sweden

⁵ Project Engineer, PEAB, Nellickevägen 22, 41263 Göteborg, Sweden

* Corresponding author, email: bengt@fellenius.net

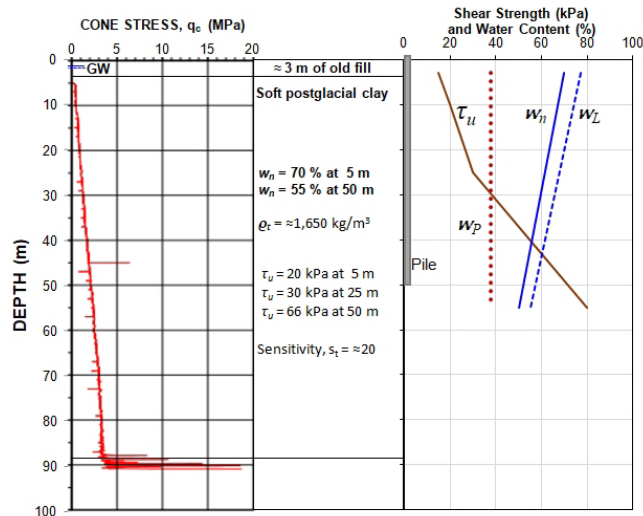


Figure 1. Soil profile

13.0 m long additional segments; total length of 50.0 m. The nominal concrete strength (cube strength) was 60 MPa. The axial reinforcement consisted of twelve 16-mm rebars placed at the cross-section corners with a 25 mm concrete cover outside a 5-mm spiral reinforcement. Each segment end to be spliced was equipped with a mechanical splice Type Leimet 270MA, consisting of a steel box cast with 6-mm thick plates covering the segment end and attached to the segment by four about 1.1 m long, 32-mm diameter rebars. Each splice corner had two diametrically opposed protruding dowels (diameter 27 mm) and two recesses.

The pile driving, was by first driving one segment and then connecting it to a second segment. Connection was made by inserting the dowels of the second segment into the recesses at surface of the first segment and vice versa. A pin was then wedged into the four dowels from the side of the splice box locking the dowels in-place to secure the splice. The pile toe, the bottom pile segment end, was slightly rounded. The pile was driven in September 2017 to 50.0-m embedment depth. An upper about 1.0 m length of the pile was free from soil contact.

All construction activities, such as pile driving, fill placement, and excavation in the area were more than 100 m away from the test pile.

The pile was strain-gage instrumented at five levels: at depths at 48.0, 32.5, 19.5, 11.0, and 2.0 m, respectively. The gages consisted of two pairs of Geokon vibrating wire Model Number 4911-4 attached to 0.91 m long, 12.7 mm diameter (#4) rebars (“sister bars”). One sister bar gage was placed at each corner of the pile inside the main reinforcement. The cables from the gages were brought out to the side of the pile and protected by a 140 mm diameter steel tube with 4 mm wall cut in half and fixed to the pile by screws. The protective tube added 70 mm to the nominal pile circumference (6%).

Gage Level, SGL5, at 2.0 m below the pile head was to serve as reference to the pile stiffness, EA ($E = \text{Young's}$

modulus and $A = \text{pile total cross sectional area}$). Because influence of shaft resistance between 1.0 m and 2.0 m depths, would be negligible, the load at that level would be the same as the load applied to the pile head. No other instrumentation, e.g., a toe telltale, was included.

The nominal pile area was 760 cm^2 and the steel area was 37 cm^2 , which includes the area of the four sister bars, spiral, and the 17 cm^2 of the protection steel tube. The circumference, including the gage-protection half-tube was 1.17 m.

During the test, a Geokon data collector Model 8032 was used to record pile head movements and strain gage records at every 2 minutes of the test.

Test Procedure

A static loading test was carried out 210 days after the driving. The test schedule was to apply 130 kN increments every 15 minutes until the pile head movement showed plunging. The pile load was applied using a 320 ton hydraulic jack with a 300 mm piston length and 121 kg mass. No load cell was included to measure the applied loads, which, therefore, were maintained from reading the pressure in the hydraulic pump. The manometer pressure was multiplied by the jack piston area to give the value of the applied load.

The reaction to the load was obtained by jacking against a beam connected to by four reaction piles placed in the corners of a 4.5 m square area with the test pile in the center. The reaction piles were similar to the test pile and each was driven to 39 m depth the day before the test pile. That is, the radial distance between test pile and reaction piles was 3.2 m. Figure 2 shows a photo of the pile head, jack, and one reaction beam. Although the reaction beam was horizontal, the test pile was not truly vertical, which required a wedge arrangement to ensure that the load would not be concentrated to the side of the test pile. This will have resulted in a horizontal force that, however, does not seem to have adversely affect the pile as the pile-head movement-gages test did not indicate any significant rotation of the pile head or bending of the pile. After the pile driving, a concrete slab was cast over the immediate area encompassing the piles. An opening



Figure 2. Photo of the set-up

in the slab was arranged around the test pile. (The slab was cast directly against the reaction piles). The reference beam was supported on the slab at about 1.5 m away from the reaction pile and about 2.5 m away from the test pile. Surveyor's leveling during the loading test confirmed that the supports of the reference beams did not heave during the test.

Test Results

When raising the load to the 14th level, 1,820 kN, movements became progressively large requiring continuous pumping to maintain the load; the pile plunged. As indicated in the jack-load vs. pile-head movement curve shown in Figure 3a, trying to maintain the load level (1,820 kN) resulted in large pile head movement and maintaining the pump pressure required that was compensated by continuous pumping. The jack-determined load reduced with the movement. Because the load measurements (jack-pressures) were affected by the jack-piston on-going movement, the load value line is drawn dashed line for at this stage of the test. Figure 3b shows the actual load-time plotted from the time stamp.

Prediction Event

Prior to the test, a widely distributed group of geotechnical engineers around the world was invited to predict the load-movement curve to be established in the test and to assess the pile capacity from this curve — a total of 22 predictions from 10 countries was received. The predicted pile-head load-movement curves are shown in Figure 4. The submitted assessments of capacity are indicated by the circles (all but two participants submitted a value of assessed capacity). The predictions of pile stiffness (initial slope of the curve) and pile head displacement showed considerable scatter. Predictions of peak load and movement at peak load ranged from 65% to 200% and 35% to 300% (excluding one outlier), respectively, of actual values, 1,800 kN and 22 mm, respectively. The few predictions who indicated a distinct peak load,

assessed the peak load as capacity. However, for those who did not predict a peak value, but assessed their predicted capacity from the curve, the values of assessed capacity ranged widely. It is obvious that the participants applied a personal definition in assessing the capacity from the respective load-movement curves, as also been found in other similar events (Fellenius, 2017).

Strain Measurements

All but one strain-gage (at SGL2, 32.5 m depth, of which pair, the records were discarded) worked well. At four levels with both pairs functioning, each pair gave about the same average. Thus, the measurements did not show any appreciable bending in the test pile. Figure 5 shows the every two-minute measurements of the four gages at SGL5, 2.0 m below the pile head (the gage levels are numbered from the deepest to the highest level in accordance with the conventional system). As shown, the averages of each pair are very close, indicating good records.

Figure 6 shows the jack load vs. strain measured for the applied load at the end of each load-holding duration, i.e., just before adding the next load increment to the pile head. The load-strain curve for SGL5, of course, is in the form of a straight line from beginning to end. Also, SGL4 to SGL2 show a straight line after an initial curved portion. The change to a straight line represents the applied load when the shaft resistance above the gage level had been fully mobilized. For example, at SGL3, the change occurred for an applied load of 750 kN and a pile head movement of about 5 mm. The fact that the straight-line portions have the same slope suggests that beyond a peak, occurring at an about 5 mm movement, the clay response is essentially plastic, that is, it appears to be neither particularly strain-hardening nor strain-softening.

The common slope represents an axial pile stiffness equal to 3.3 GN. A more accurate method of determining

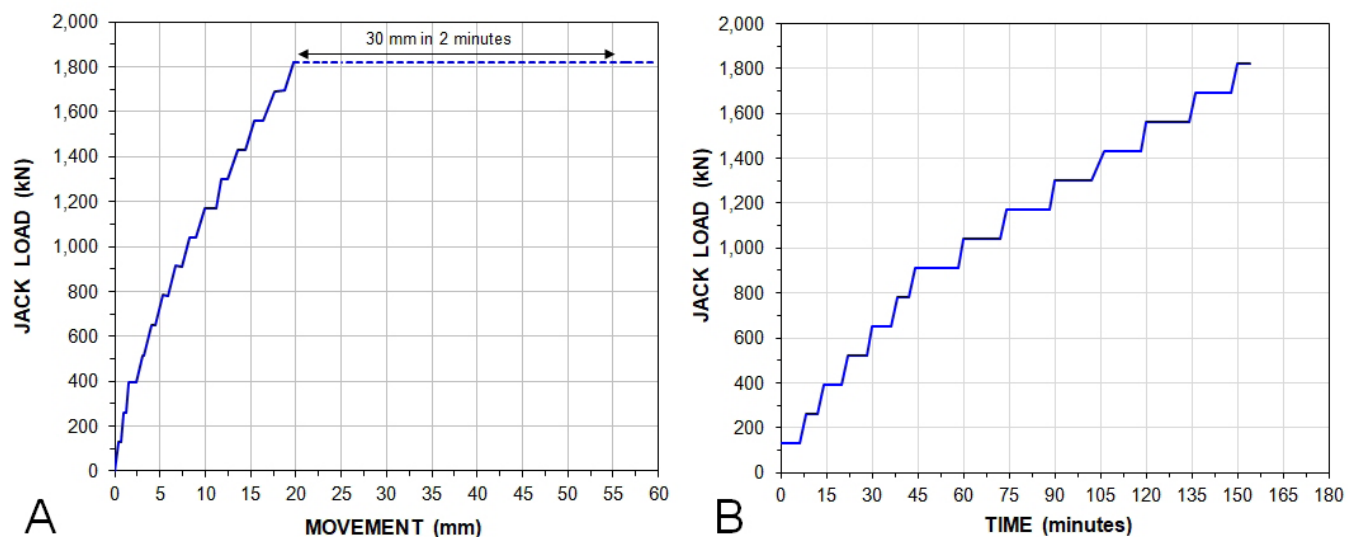


Figure 3. (a) Jack load vs. pile head movement and (b) jack load vs. time

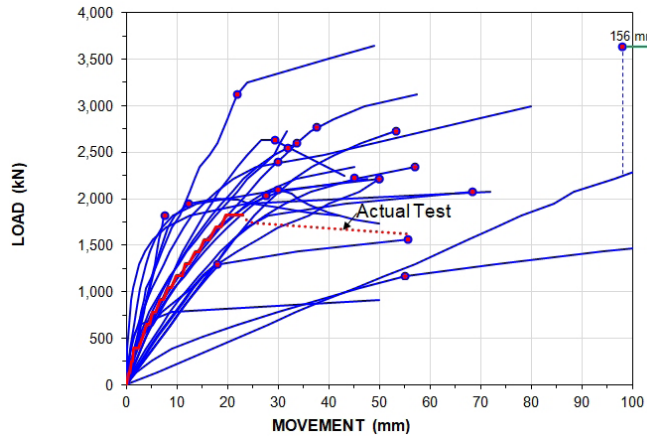


Figure 4. Predicted load-movement curves and assessed capacities received from the 22 individuals participating in the prediction event

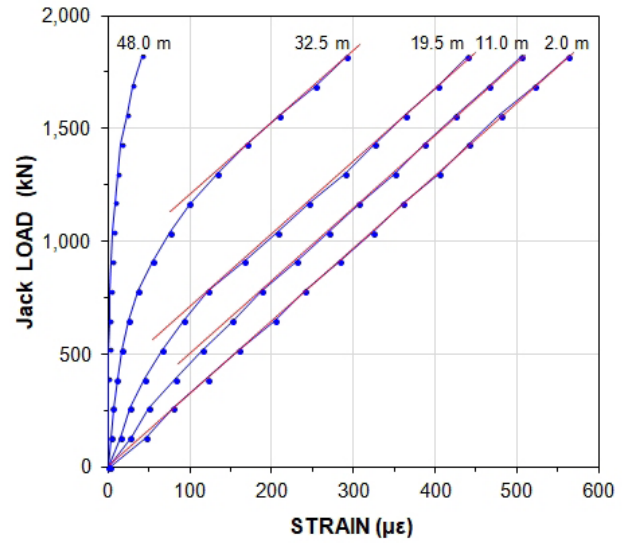


Figure 6. Load-strain measured for the last reading of each load level for the five gage levels

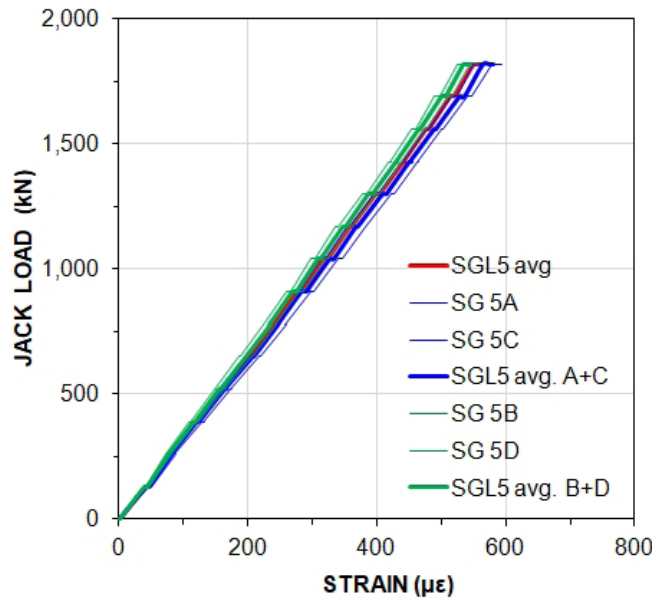


Figure 5. Load-strain measurements at SGL5, 2 m below the pile head.

the pile stiffness is using the direct secant slope (stiffness) method, which applies to a gage level close to the pile head, and the tangent slope (stiffness) method, which applies to any gage level. The direct secant method is a plot of load divided by strain versus strain as shown in Figure 7a applied to Gage Level 5. The tangent method applies to all five gage levels. It addresses change of load over change of strain versus strain as shown in Figure 7b. The methods indicate a pile stiffness, EA/L , of 3.25 GN/m, which reduced with increasing strain, though only to a negligible degree. Applying the nominal pile cross sectional area ($A = 0.0756 \text{ m}^2$), shows a 42.0 GPa E-modulus of the concrete and steel reinforcement combination. Separated on areas of reinforcement ($E_{\text{steel}} = 207 \text{ GPa}$) and concrete, the E_{concrete} is 34.3 GPa. The conventional relation for E_{concrete} applied in Sweden is $E_{\text{concrete}} = 5,000\sqrt{\sigma_{\text{strength}}}$

(MPa), which for the 60 MPa nominal strength indicates an E_{concrete} value of 39 GPa, i.e., a 13% overestimation.

The load at each gage level for each load applied to the pile head was determined by multiplying the measured strains with the evaluated stiffness. The load-movement curves in Figure 8 show the so-calculated loads versus movement for the five gage levels. The simulated curves show load-movements at the gage level to a 30-mm calculated pile-toe movement. Before the maximum load was reached, the values of applied load and the load determined from the uppermost strain-gage agreed well, indicating that the strain-gage functioned as a load cell. The measured loads are approximate after the peak load—the jack load because of the moving piston and the loads calculated from the strain values because the axial load changed during the gage stabilization time (a few seconds per gage reading) affecting the strain-values—not so much within each gage level as between gage levels.

The curves indicate a small strain-softening effect for movement beyond the maximum resistance. The red, solid lines are simulated load-movement curves fitted to the test data using a Zhang $t-z$ function (Fellenius, 2020) as shown in Figure 9, indicating a slight strain-softening response. To achieve the fit, the toe resistance had to be very small: 15 kN ($\approx 200 \text{ kPa}$) for 5 mm movement. The toe function ($q-z$) was a Gwizdala function with a function coefficient, θ , equal to 0.40, which corresponds to a unit toe resistance, $r_s \approx 500 \text{ kPa}$ at a 25mm toe movement. A θ coefficient of 0.5 or smaller is commensurate with residual toe force condition where the pile toe stress has relaxed from an earlier larger stress typical of driven piles.

The simulations shown in Figure 8 applied effective stress analysis (“beta-method”) and the same $t-z$ function was applied to all five gage levels. However, to achieve the fit between measured and simulated values, taking the maximum load as the Target Load for the analysis, the shear

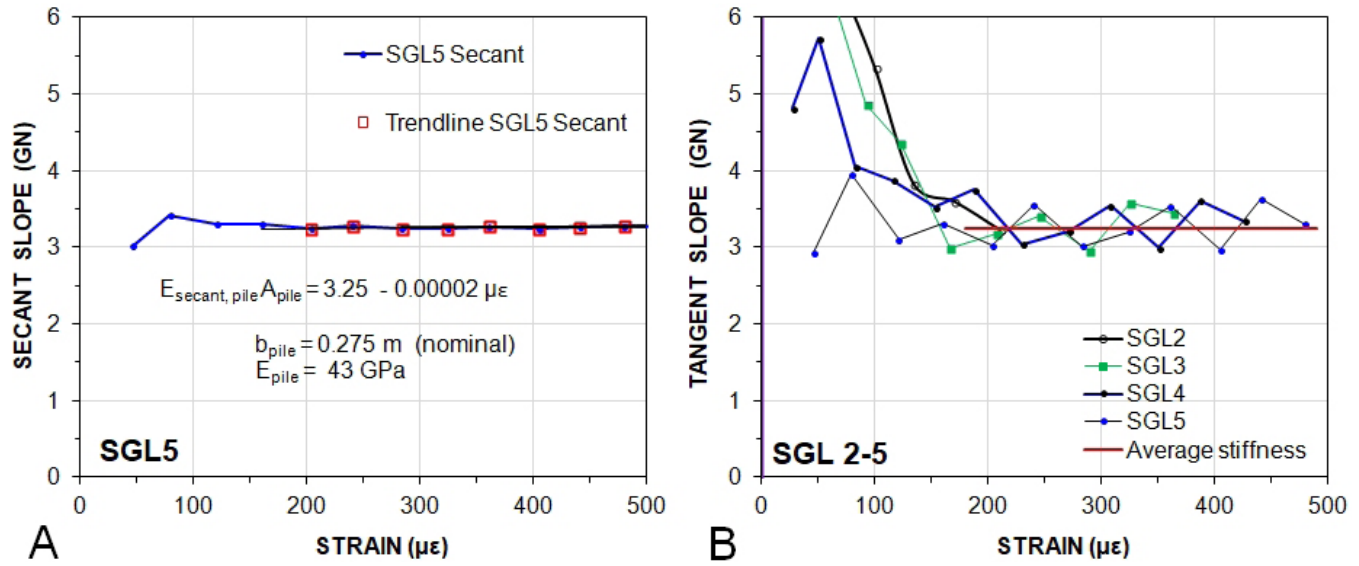


Figure 7. (a) Secant axial stiffness at SGL5 and (b) tangent axial stiffness at all gage levels

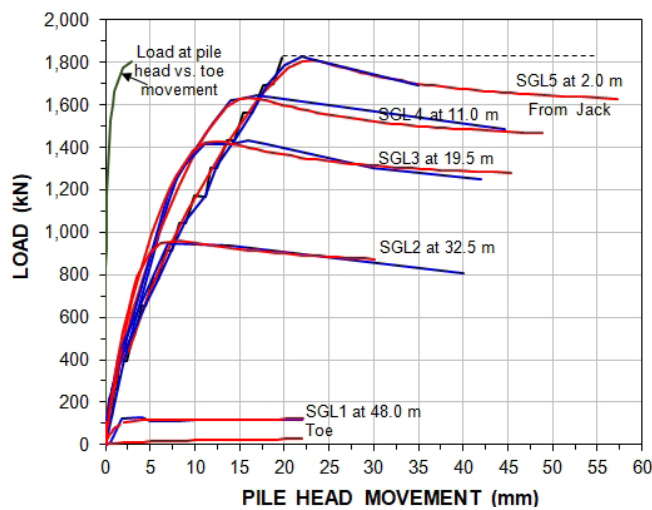


Figure 8. Measured and simulated load-movement curves

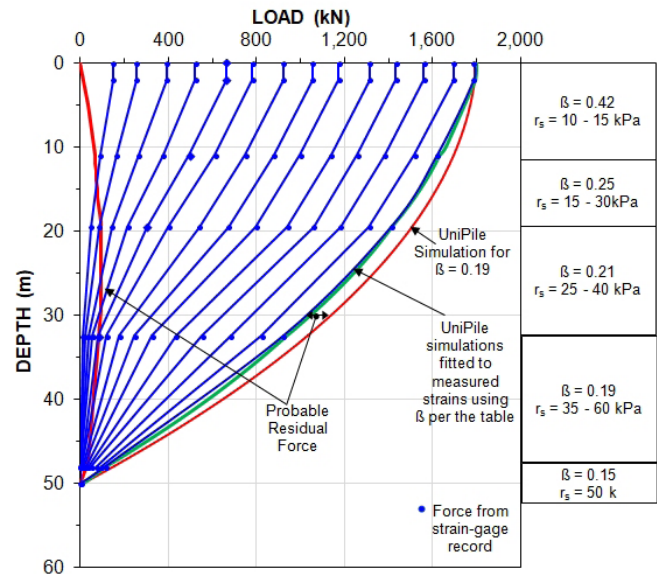


Figure 10. Distribution of applied loads and probable residual force

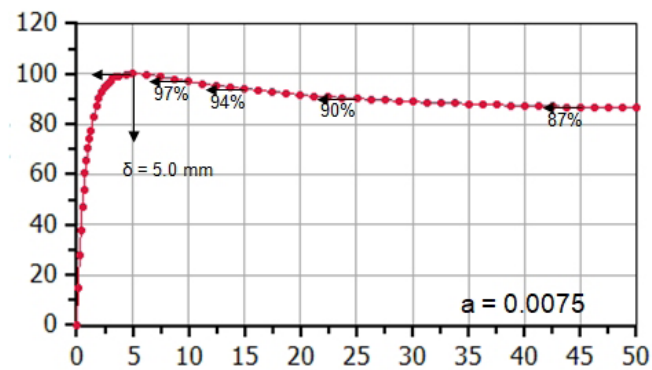


Figure 9. The Zhang t - z function applied to the records from the five gage levels

resistances at the gage levels differed (expressed as a beta-coefficient for the maximum element force), as indicated in Figure 10.

Figure 10 shows the array of load distributions analyzed for all records up to the maximum load applied and the latter curve is also shown as simulated (fitted) using UniPile. This fit required reducing the beta-coefficients with depth from $\beta = 0.42$ through $\beta = 0.15$. However, it is unlikely that coefficient would reduce with depth in this homogenous clay, the figure also includes a fit for with a constant beta-coefficient ($\beta = 0.19$), which is probably closer to the true fit. The reason for the discrepancy is that the measured strains do not include the force, called “residual force”, present in the pile at the

start of the test. The difference between the two curves is the distribution of the residual force.

The residual force shown in Figure 10 compares well with actually measured residual force in a similar pile installed about 5 km away from the site, a hexagonal 300 mm diameter pile (H800) driven through 40 m of a very similar, though slightly softer clay as that at the current test site and into an underlying sand (Fellenius 1972). The purpose of the H800-pile study was to measure development of negative skin friction and drag force with time. However, the concept of residual force and drag force are identical. The term “residual force” applies when the force is present in a pile at the start of a static loading test, whereas “drag force” is the term to use when the force develops after a structure is placed on the pile(s).

The nominal circumferences of the two piles are 1.17 m and 1.06 m, respectively. The probable distribution of residual force in the current pile and the distribution of residual force actually measured in the H800 pile are plotted together in Figure 11. Down to a depth of about 20 m, the two distributions agreed well. Below 20 m, for the current pile, the force first became constant and then reduced for the rest of the pile length, whereas the force in the H800 continued to increase all through the clay layer before decreasing in the sand. This difference is due to the fact that a residual force starts to reduce by gradually progressing from negative to positive directions in a transition zone, establish-

ing the force-equilibrium neutral-plane for the axial force in the pile. The much larger resistance for the in-sand portion of the H800 pile caused the neutral plane to be developed deeper down than for the current test pile due to the larger shaft and toe resistances of the H800 pile mobilized in the sand below 40 m depth. The partially mobilized shaft resistance for 200 days set-up correlates to a beta-coefficient of about 0.10. The residual force is due to the reconsolidation (pore pressure dissipation and its associated soil movement) of the clay after the driving. The movement associated with the build-up of the residual force must have been very small because, as the loading test indicated, full mobilization required less than 5 mm of movement (c.f., Figure 9), which also was found to be the case for the H800 pile study. Because of the very small movement, the residual force is not fully mobilized.

Conclusions

This paper summarizes the static load test on a 50 m long, strain-gage instrumented, square 275-mm diameter, precast, shaft-bearing (“floating”) pile in Göteborg, Sweden. The head-down static-loading test reached an 1,800-kN maximum load for 22-mm pile-head movement and 3-mm pile toe movement, with about 20 mm difference being pile compression.

The analysis of the strain-gage records using the secant and tangent stiffness methods indicated a 3.25-GN pile stiffness, EA, that correlated to a concrete E-modulus of 34.3 GPa.

The evaluation of the strain-determined loads versus movement showed a good fit to a Zhang t-z function for a 5 mm movement and a 0.0075 function coefficient. The toe resistance in the soft clay was very small, only about 200 kPa at 3 mm movement increasing to about 500 kPa at 25 mm movement per a Gwizdala q-z function with a function coefficient of 0.4.

The maximum test load for the 50-m long pile occurred for plastic shaft resistance and correlated to an effective stress analysis with a constant beta-coefficient of 0.19. Fitting the load distribution for each strain-gage level separately indicated a beta-coefficient that reduced with depth. This is because that at the start of the loading test, residual force due to reconsolidation and pore pressure dissipation had developed in the pile. The residual force distribution was estimated, and the distribution compared well to that found in earlier measurements of residual force for the Göteborg region. Prior to the test, geotechnical engineers around the world were invited to predict the load-displacement curve of the pile specimen describe above. The competition entries consisted of 22 predictions from 10 countries. The predictions of pile stiffness, and pile head displacement showed considerable scatter. Predicted peak loads ranged from 65% to 200% of the actual 1,800-kN peak-load, and 35% to 300% of the load at 22-mm movement. The assessment of capacity from the predicted curve showed clearly that the definition of “capacity” varies considerably in the profession.

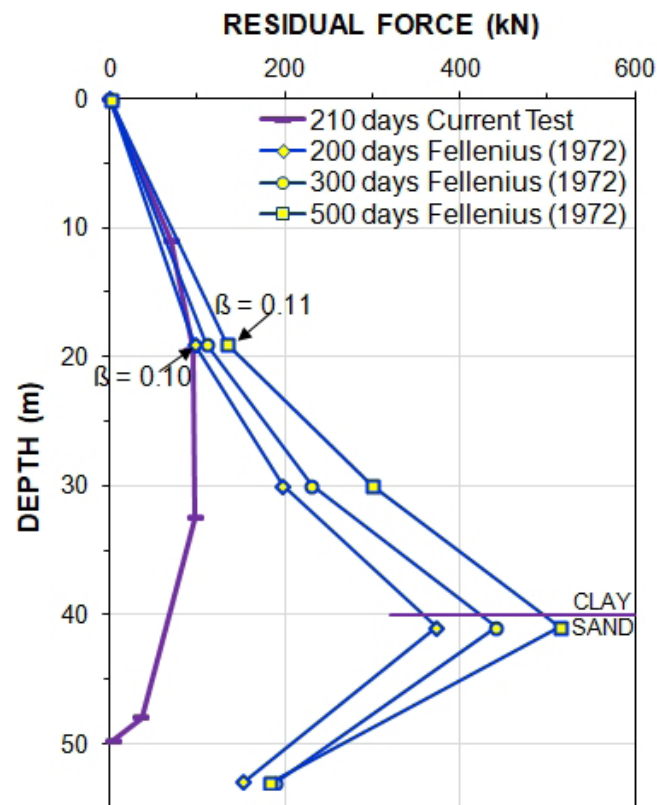


Figure 11. Residual force compared to previous measurements

References

- Edvardsson, F. & Pettersson J., 2018. *Geotechnical response of an axially loaded floating pile in soft soil*. Chalmers University of Technology, Dept. of Civil Engineering, M.Eng. Thesis. 155 p., retrieved from <http://publications.lib.chalmers.se/records/fulltext/255659/255659.pdf>
- Fellenius, B.H. (1972). Downdrag on piles in clay due to negative skin friction. *Canadian Geotechnical Journal*, 9(4), 323-337.
- Fellenius, B.H. (2017). Report on the B.E.S.T. prediction survey of the 3rd CBFP event. *Proceedings of the 3rd Bolivian International Conference on Deep Foundations*, Santa Cruz de la Sierra, Bolivia, April 27-29, Vol. 3, pp. 7-25.
- Fellenius, B.H. (2020). *Basics of foundation design*. Electronic Edition, retrieved from www.Fellenius.net, 524 p.